# Modeling and Control Design of a Robotic Sailboat

Hadi Saoud, Minh-Duc Hua, Frédéric Plumet, and Faïz Ben Amar

**Abstract.** This paper presents a method to obtain a full 6 degrees of freedom dynamic model of a robotic sailing boat starting from the description of forces and torques acting on it. A general 6-DOF model is first described and then simplified to obtain a 3-DOF control-oriented one. Relying on it, a rudder controller and a sail's trimming calculator are proposed. This controller has been validated using a numerical implementation of the proposed dynamic model.

## 1 Introduction

Thanks to their low energy consumption, autonomous sailing robots provide a promising solution for long-term missions and semi-persistent presence in the oceans and a lot of sailing robot projects have been launched recently all around the world [1, 3, 3, 4, 6, 8, 10, 12]. However, the nature of sailing boats implies restrictions on their navigation capabilities: thrust forces depend on uncontrollable and partially unpredictable wind. Furthermore, such vehicles exhibit complex behavior due to aero and hydrodynamic properties of sails and hull. Therefore, in order to improve the control of sailboats, a model reflecting the dynamic of the system and its relation with physical phenomenon (wind speed and marine current) is necessary.

One of the contributions of the present paper is the proposition of a simple but representative model for control design and also for the validation of the proposed controllers via simulation means.

The paper is organized as follow: first, the sailboat is divided into three subsystems (hull, mainsail and rudder) and the forces and torques acting

Hadi Saoud · Minh-Duc Hua · Frédéric Plumet · Faïz Ben Amar
Institut des Systèmes Intelligents et de Robotique (ISIR),
UPMC Université Paris 6, CNRS-UMR 7222, France
e-mail: {saoud,hua,plumet,amar}@isir.upmc.fr

F. Le Bars and L. Jaulin (eds.), *Robotic Sailing 2013*, 
DOI: 10.1007/978-3-319-02276-5_8, 

on each subsystem are described. Then, a general 6-DOF similar to [5] is proposed. Some assumptions are made to simplify the model to a 4-DOF one with roll and yaw as in [16]. For control design, a more simplified 3-DOF model without roll is proposed. Analysis of this model leads to the definition of a new heading controller using backstepping control method [7] with variable gains and a sail's trimming algorithm, both presented in the last section of this paper.

A numerical implementation of the 3-DOF model and controllers is done and some simulation results are presented.

## 2 Notation

- For any $x \in \mathbb{R}^{m\times n}$, $x^\top$ denotes the transpose of $x$ and $\dot{x}$ its time-derivative.
- $\overrightarrow{x}$ denotes an affine vector associated with the vector space $x \in \mathbb{R}^3$.
- The scalar product of two vectors $\overrightarrow{x}$ and $\overrightarrow{y}$ is denoted as $\overrightarrow{x}.\overrightarrow{y}$, and their cross product as $\overrightarrow{x} \times \overrightarrow{y}$.
- $\{e_1, e_2, e_3\}$ denotes the canonical basis of $\mathbb{R}^3$. The Euclidean norm is denoted as $|\cdot|$.
- For any $x \in \mathbb{R}^3$, the notation $x_\times$ denotes the skew-symmetric matrix associated with $x$, i.e. $x_\times y = x \times y$, $\forall y \in \mathbb{R}^3$.
- For any affine vector $\overrightarrow{x}$ and any frame $\mathcal{X}$, $x^{\mathcal{X}}$ denotes the vector of coordinates of $\overrightarrow{x}$ in the basis of the frame $\mathcal{X}$.
- $R^{\mathcal{Y}}_{\mathcal{X}} \in SO(3)$ denotes the rotation matrix representing the orientation of the frame $\mathcal{X}$ with respect to (w.r.t.) the frame $\mathcal{Y}$. For any affine vector $\overrightarrow{x}$, one verifies $x^{\mathcal{Y}} = R^{\mathcal{Y}}_{\mathcal{X}} x^{\mathcal{X}}$.
- $G$: sailboat's center of mass (CoM).
- $G_s$, $G_r$, $G_k$: center of pressure of the sail, the rudder and the keel, all assumed to be fixed.
- $\mathcal{I} = \{0; \overrightarrow{\imath}_0, \overrightarrow{\jmath}_0, \overrightarrow{k}_0\}$: Inertial frame chosen as the North-West-Up frame.
- $\mathcal{B} = \{G; \overrightarrow{\imath}, \overrightarrow{\jmath}, \overrightarrow{k}\}$: Body frame fixed to the hull.
- $\mathcal{S} = \{G_s; \overrightarrow{\imath}_s, \overrightarrow{\jmath}_s, \overrightarrow{k}_s\}$: Sail-fixed frame.
- $\mathcal{R} = \{G_r; \overrightarrow{\imath}_r, \overrightarrow{\jmath}_r, \overrightarrow{k}_r\}$: Rudder-fixed frame, with $\overrightarrow{k} \equiv \overrightarrow{k}_s \equiv \overrightarrow{k}_r$.
- $m_0 \in \mathbb{R}$, $J_0 \in \mathbb{R}^{3\times 3}$: sailboat's mass and inertia matrix.
- $\overrightarrow{x}$, $\overrightarrow{x}_s$, $\overrightarrow{x}_r$: position of $G$, $G_s$ and $G_r$ w.r.t. the inertial frame.
- $\overrightarrow{\omega}$: angular velocity of the body-fixed frame w.r.t. the inertial frame.
- $\overrightarrow{v}$: linear velocity of $G$ w.r.t. the inertial frame.
- $\overrightarrow{v}_s$, $\overrightarrow{v}_r$, $\overrightarrow{v}_k$: linear velocity of $G_s$, $G_r$ and $G_k$ w.r.t. the inertial frame.
- $\overrightarrow{v}_w$: wind velocity w.r.t. the inertial frame.
- $\overrightarrow{v}_c$: water current velocity w.r.t. the inertial frame.
- $\overrightarrow{v}_{as}$, $\overrightarrow{v}_{ar}$, $\overrightarrow{v}_{ak}$: apparent velocity of the sail, the rudder and the keel.
- $x$, $R$, $\omega$, $v$: short notation of $x^{\mathcal{I}}$, $R^{\mathcal{I}}_{\mathcal{B}}$, $\omega^{\mathcal{B}}$, $v^{\mathcal{B}}$, respectively.
- $\nu := [v, \omega]^\top$.

- $\delta_s$, $\delta_r$: sail's angle and rudder's angle, respectively.
- $\alpha_s$: sail's angle of attack.
- $\alpha_r$: rudder's angle of attack.
- $\alpha_k$: keel's angle of attack.
- $S_s$, $S_r$, $S_k$: surface of the sail, rudder and keel, respectively.
- $\rho_{air}$, $\rho_{water}$: air and water density, respectively.
- $C_s^L(\cdot)$, $C_s^D(\cdot)$: lift and drag coefficients of the sail, respectively.
- $C_r^L(\cdot)$, $C_r^D(\cdot)$: lift and drag coefficients of the rudder, respectively.
- $C_k^L(\cdot)$, $C_k^D(\cdot)$: lift and drag coefficients of the keel, respectively.

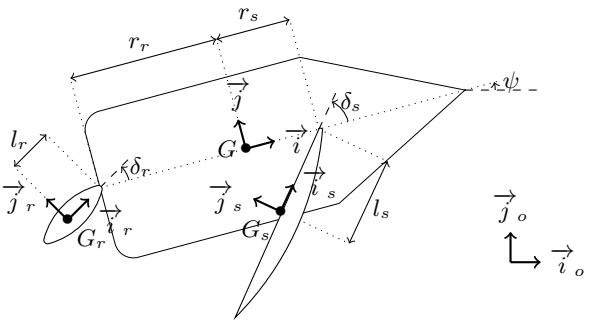


**Fig. 1** Notation

## 3 System Modeling

### *3.1 Forces And Torques Acting on the System*

The sailboat under consideration can be divided into three rigid parts: a sail, a rudder, and a main body composed of a keel and a hull. In what follows, the modeling of forces and torques acting on the sailboat is presented.

#### 3.1.1 Aerodynamic Forces and Torques Acting on the Sail

Interactions between a rigid body and the surrounding fluid are governed by the Navier–Stocks equations. In the first approximation, the aerodynamic forces $\overrightarrow{F}_s$ acting on the sail can be expressed by a function dependent upon the constant air density $\rho_{air}$, the Reynolds number $R_e$ and the angle of attack $\alpha_s$. The latter variable is the angle between the apparent velocity $\overrightarrow{v}_{as}$ of the sail (defined as the difference between the velocity of $G_s$ and the wind

velocity $\overrightarrow{v}_w$, i.e. $\overrightarrow{v}_{as} := \overrightarrow{v}_s - \overrightarrow{v}_w$) and the zero-lift line which coincides with the orthogonal projection of $\overrightarrow{v}_{as}$ onto the sail's plane.

First, let us derive the expression of the velocity $\overrightarrow{v}_s$ of $G_s$. Using the relations $\overrightarrow{GG_s} = r_s \overrightarrow{\imath} - l_s \overrightarrow{\imath}_s + h_s \overrightarrow{k}$ and $\overrightarrow{x}_s = \overrightarrow{x} + \overrightarrow{GG_s}$, one obtains the following relation expressed in the inertial frame:

$$x_s^{\mathcal{I}} = x + R(r_s e_1 + h_s e_3 - l_s R_{\mathcal{S}}^{\mathcal{B}} e_1)$$

Differentiating both sides of the above equation w.r.t. time, one gets:

$$\begin{aligned} & Rv_s^{\mathcal{B}} = Rv + R\omega_\times (r_s e_1 + h_s e_3 - l_s R_{\mathcal{S}}^{\mathcal{B}} e_1) - l_s \dot{\delta}_s R R_{\mathcal{S}}^{\mathcal{B}} e_3 \times e_1 \\ \Rightarrow \quad & v_s^{\mathcal{B}} = v + \omega_\times (r_s e_1 + h_s e_3 - l_s R_{\mathcal{S}}^{\mathcal{B}} e_1) - l_s \dot{\delta}_s R_{\mathcal{S}}^{\mathcal{B}} e_2 \end{aligned}$$

which also yields in the form of affine vectors:

$$\overrightarrow{v}_s = \overrightarrow{v} + \overrightarrow{\omega} \times \overrightarrow{GG_s} - l_s \dot{\delta}_s \overrightarrow{\jmath}_s$$

Consequently, the expression of the apparent velocity of the sail satisfies:

$$\overrightarrow{v}_{as} = \overrightarrow{v} - \overrightarrow{v}_w + \overrightarrow{\omega} \times \overrightarrow{GG_s} - l_s \dot{\delta}_s \overrightarrow{\jmath}_s$$

From here, the sail's angle of attack can be computed as:

$$\alpha_s := \operatorname{atan}\left(\frac{-\overrightarrow{v}_{as}.\overrightarrow{\jmath}_s}{\sqrt{(\overrightarrow{v}_{as}.\overrightarrow{\imath}_s)^2 + (\overrightarrow{v}_{as}.\overrightarrow{k}_s)^2}}\right) = \operatorname{atan}\left(\frac{-v_{as,2}^{\mathcal{S}}}{\sqrt{(v_{as,1}^{\mathcal{S}})^2 + (v_{as,3}^{\mathcal{S}})^2}}\right)$$

The aerodynamic force vector $\overrightarrow{F}_s$ can be decomposed in two components: the lift force $\overrightarrow{F}_s^L$, perpendicular to the apparent velocity, and the drag force, parallel to the apparent velocity. The lift force direction is characterized by the unit vector $\overrightarrow{e}_s^L := \sin\alpha_s \overrightarrow{\beta}_s + \cos\alpha_s \overrightarrow{\jmath}_s$, where $\overrightarrow{\beta}_s$ is the unit vector collinear with the vector $\overrightarrow{v}_{as,1,3} := (\overrightarrow{v}_{as}.\overrightarrow{\imath}_s)\overrightarrow{\imath}_s + (\overrightarrow{v}_{as}.\overrightarrow{k}_s)\overrightarrow{k}_s$. Besides, since the apparent velocity $\overrightarrow{v}_{as}$ can be expressed in the form $\overrightarrow{v}_{as} = |\overrightarrow{v}_{as}|(\cos\alpha_s \overrightarrow{\beta}_s - \sin\alpha_s \overrightarrow{\jmath}_s)$, one easily deduces that: From here, the aerodynamic lift and drag forces can be modeled as:

$$\begin{cases} \overrightarrow{F}_s^D = -\lambda_s C_s^D(\alpha_s)|\overrightarrow{v}_{as}|\overrightarrow{v}_{as} \\ \overrightarrow{F}_s^L = \lambda_s C_s^L(\alpha_s)|\overrightarrow{v}_{as}|^2 \overrightarrow{e}_s^L = \lambda_s C_s^L(\alpha_s)|\overrightarrow{v}_{as}|\left(\tan\alpha_s \overrightarrow{v}_{as} + \dfrac{|\overrightarrow{v}_{as}|}{\cos\alpha_s}\overrightarrow{\jmath}_s\right) \end{cases}$$

with $\lambda_s := \frac{1}{2}\rho_{air} S_s$, $C_s^L(\alpha_s)$ the lift coefficient and $C_s^D(\alpha_s) > 0$ the drag coefficient. Thus, the expression of the total resulting aerodynamic force $\overrightarrow{F}_s := \overrightarrow{F}_s^D + \overrightarrow{F}_s^L$ satisfies:

$$\overrightarrow{F}_s = -\lambda_s \left(C_s^D(\alpha_s) - C_s^L(\alpha_s)\tan\alpha_s\right) |\overrightarrow{v}_{as}|\overrightarrow{v}_{as} + \lambda_s \frac{C_s^L(\alpha_s)}{\cos\alpha_s}|\overrightarrow{v}_{as}|^2\overrightarrow{\jmath}_s \quad (1)$$

Finally, one deduces the resulting torque vector:

$$\overrightarrow{\tau}_s = \overrightarrow{GG_s} \times \overrightarrow{F}_s \quad (2)$$

The above deduction can be directly applied to obtain the expressions of the hydrodynamic forces and torques acting on the rudder and the keel.

### 3.1.2 Hydrodynamic Forces and Torques Acting on the Rudder

Similarly to the previous case, one deduces that the velocity of $G_r$ satisfies $\overrightarrow{v}_r = \overrightarrow{v} + \overrightarrow{\omega} \times \overrightarrow{GG_r} - l_r\dot{\delta}_r\overrightarrow{\jmath}_r$, with $\overrightarrow{GG_r} = -r_r\overrightarrow{\imath} - l_r\overrightarrow{\imath}_r - h_r\overrightarrow{k}$. Subsequently, the apparent velocity of the rudder, defined as $\overrightarrow{v}_{ar} := \overrightarrow{v}_r - \overrightarrow{v}_c$, is given by:

$$\overrightarrow{v}_{ar} = \overrightarrow{v} - \overrightarrow{v}_c + \overrightarrow{\omega} \times \overrightarrow{GG_r} - l_r\dot{\delta}_r\overrightarrow{\jmath}_r \quad (3)$$

Then, similarly to the sail case, the total hydrodynamic force acting on the rudder can be modeled as:

$$\overrightarrow{F}_r = -\lambda_r \left(C_r^D(\alpha_r) - C_r^L(\alpha_r)\tan\alpha_r\right) |\overrightarrow{v}_{ar}|\overrightarrow{v}_{ar} + \lambda_r \frac{C_r^L(\alpha_r)}{\cos\alpha_r}|\overrightarrow{v}_{ar}|^2\overrightarrow{\jmath}_r \quad (4)$$

with $\lambda_r = \frac{1}{2}\rho_{water}S_r$, $C_r^L(\alpha_r)$ the lift coefficient, $C_r^D(\alpha_r) > 0$ the drag coefficient and $\alpha_r$ the rudder's angle of attack defined as:

$$\alpha_r := \text{atan}\left(-v_{ar,2}^{\mathcal{R}}/\sqrt{(v_{ar,1}^{\mathcal{R}})^2 + (v_{ar,3}^{\mathcal{R}})^2}\right)$$

Finally, the resulting torque vector is:

$$\overrightarrow{\tau}_r = \overrightarrow{GG_r} \times \overrightarrow{F}_r \quad (5)$$

### 3.1.3 Hydrodynamic Forces and Torques Acting on the Keel

Since the keel is rigidly attached to the sailboat's hull and its $x$-axis coincides with the one of the vehicle, one deduces that the apparent velocity of the keel satisfies:

$$\overrightarrow{v}_{ak} = \overrightarrow{v} - \overrightarrow{v}_c + \overrightarrow{\omega} \times \overrightarrow{GG_k}$$

with $\overrightarrow{GG_k} = -h_k\overrightarrow{k}$. The keel's angle of attack is defined as:

$$\alpha_k := \text{atan}\left(-v_{ak,2}^{\mathcal{B}}/\sqrt{(v_{ak,1}^{\mathcal{B}})^2 + (v_{ak,3}^{\mathcal{B}})^2}\right)$$

Similarly to the sail and rudder case, the total hydrodynamic force acting on the keel is given by:

$$\overrightarrow{F}_k = -\lambda_k \left(C_k^D(\alpha_k) - C_k^L(\alpha_k)\tan\alpha_k\right) |\overrightarrow{v}_{ak}|\overrightarrow{v}_{ak} + \lambda_k \frac{C_k^L(\alpha_k)}{\cos\alpha_k}|\overrightarrow{v}_{ak}|^2\overrightarrow{\jmath} \quad (6)$$

with $\lambda_k = \frac{1}{2}\rho_{water}S_k$. Finally, the resulting torque vector is:

$$\overrightarrow{\tau}_k = \overrightarrow{GG_r} \times \overrightarrow{F}_k \quad (7)$$

### 3.1.4 Hydrodynamic Resistance Forces and Torques

Hydrodynamic resistance is caused by the friction and the waves. In the first approximation, the resistance force on the hull can be modeled as the sum of linear and quadratic terms:

$$\begin{aligned}\overrightarrow{F_d} = &- c_1^\imath(\overrightarrow{v}_a \cdot \overrightarrow{\imath})^2 \cdot \overrightarrow{\imath} - c_2^\imath(\overrightarrow{v}_a \cdot \overrightarrow{\imath})\overrightarrow{\imath} - c_1^\jmath(\overrightarrow{v}_a \cdot \overrightarrow{\jmath})^2 \cdot \overrightarrow{\jmath} - c_2^\jmath(\overrightarrow{v}_a \cdot \overrightarrow{\jmath})\overrightarrow{\jmath} \\ &- c_1^k(\overrightarrow{v}_a \cdot \overrightarrow{k})^2 \cdot \overrightarrow{k} - c_2^k(\overrightarrow{v}_a \cdot \overrightarrow{k})\overrightarrow{k}\end{aligned}$$

with $\overrightarrow{v}_a := \overrightarrow{v} - \overrightarrow{v}_c$. A similar form for the resistance torque generated by rotational movement is:

$$\overrightarrow{\tau_d} = -c_3^\imath\omega_1^2\overrightarrow{\imath} - c_4^\imath\omega_1\overrightarrow{\imath} - c_3^\jmath\omega_2^2\overrightarrow{\jmath} - c_4^\jmath\omega_2\overrightarrow{\jmath} - c_3^k\omega_3^2\overrightarrow{k} - c_4^k\omega_3\overrightarrow{k}$$

Translation resistance coefficients along $\overrightarrow{\jmath}$ and $\overrightarrow{k}$ are higher than along $\overrightarrow{\imath}$, making damping more important on lateral movement. This is due to the shape of the hull (its length is more important than its height or width). For the same reason, rotational resistance coefficients around $\overrightarrow{\jmath}$ and $\overrightarrow{k}$ are less than around $\overrightarrow{\imath}$.

### 3.1.5 Restoring Force and Torque Acting on the Hull

Let $\nabla$ be the displacement volume of water, $B$ the center of buoyancy and $M$ the ship metacenter, $\overrightarrow{F}_B$ the buoyancy force and $\overrightarrow{F}_G$ the gravity one. The restoring force and torque can be modeled as (see e.g. [5]):

$$\overrightarrow{F}_{res.} = \overrightarrow{F}_G + \overrightarrow{F}_B = -mg\overrightarrow{k}_0 + \nabla\rho_{water}\overrightarrow{k}_0$$

$$\overrightarrow{\tau}_{res.} = \overrightarrow{F_B} \times \overrightarrow{GB} = \overrightarrow{F_B} \times (\overrightarrow{GM} + \overrightarrow{GB}) = \overrightarrow{F_B} \times \overrightarrow{GM}$$

where the last equality is obtained under the approximation $\overrightarrow{k}_0 \times \overrightarrow{MB} \approx \overrightarrow{0}$.

## *3.2 Rigid-Body Equations of Motion*

### 3.2.1 General 6-DOF Equations of Motion

The kinematic equations of motion of the sailboat are given by:

$$\begin{cases} \dot{x} = Rv \\ \dot{R} = R\omega_\times \end{cases} \tag{8}$$

For modeling the dynamics of the sailboat, the added mass effects are also taken into account. Some definitions are recalled (see, e.g., [5]). Since the center of mass $G$ coincides with the origin of the body-fixed frame $\mathcal{B}$, the rigid-body inertia matrix $M_{RB}$ and the Coriolis and centripetal rigid-body matrix $C_{RB}(\nu)$ have the following form [5]:

$$M_{RB} := \begin{bmatrix} mI_3 & 0 \\ 0 & J_0 \end{bmatrix}, \quad C_{RB}(\nu) := \begin{bmatrix} m\omega_\times & 0 \\ 0 & -(J_0\omega)_\times \end{bmatrix}$$

The added inertia and Coriolis/centripetal added matrices are denoted as [5]:

$$M_A := \begin{bmatrix} A_{11} & A_{12} \\ A_{21} & A_{22} \end{bmatrix}, \quad C_A(\nu) := \begin{bmatrix} 0 & -(A_{11}v + A_{12}\omega)_\times \\ -(A_{11}v + A_{12}\omega)_\times & -(A_{21}v + A_{22}\omega)_\times \end{bmatrix}$$

Let us also define $M_T := M_{RB} + M_A$ and $C_T(\nu) := C_{RB}(\nu) + C_A(\nu)$. From here, the general 6 DOF dynamic equations of motion are given by [5]:

$$M_T\dot{\nu} + C_T(\nu)\nu = \begin{bmatrix} F_d^{\mathcal{B}} + F_{res.}^{\mathcal{B}} + F_s^{\mathcal{B}} + F_r^{\mathcal{B}} + F_k^{\mathcal{B}} \\ \tau_d^{\mathcal{B}} + \tau_{res.}^{\mathcal{B}} + \tau_s^{\mathcal{B}} + \tau_r^{\mathcal{B}} + \tau_k^{\mathcal{B}} \end{bmatrix} \tag{9}$$

We now simplify the expressions of lift and drag forces and torques acting on the sailboat by assuming that the lift and drag coefficients of the sail, the rudder and the keel satisfy the relation:

$$C_i^D(\alpha_i) - C_i^L(\alpha_s)\tan(\alpha_i) = c_0^i, \quad i = s, r, k \tag{10}$$

with $c_0^i$ some very small positive numbers, i.e. $c_0^i \ll 1$. An exemplified model for which relation (10) holds is (11), which is convenient for NACA 00XX profiles [11].

$$\begin{cases} C_i^D(\alpha_i) = c_0^i + 2c_1^i \sin^2(\alpha_i) \\ C_i^L(\alpha_i) = c_1^i \sin(2\alpha_i) \end{cases} \tag{11}$$

with $c_0^i, c_1^i$ some positive parameters. This lift and drag coefficients model can be used for sails, rudder and keel and remains convenient for control and design purpose although it neglects the stall phenomenon. For modeling purpose, more accurate sails models can be used as [15]. From here, using Eqs. (1), (4), (6) and model (11), one deduces:

$$\begin{cases} F_s^{\mathcal{B}} \approx \lambda_s \dfrac{C_s^L(\alpha_s)}{\cos\alpha_s} |\overrightarrow{v}_{as}|^2 R_{\mathcal{S}}^{\mathcal{B}} e_2 = 2\lambda_s c_1^s |v_{as}^{\mathcal{S}}| v_{as,2}^{\mathcal{S}} (\sin\delta_s e_1 - \cos\delta_s e_2) \\ F_r^{\mathcal{B}} \approx \lambda_r \dfrac{C_r^L(\alpha_r)}{\cos\alpha_r} |\overrightarrow{v}_{ar}|^2 R_{\mathcal{R}}^{\mathcal{B}} e_2 = 2\lambda_r c_1^r |v_{ar}^{\mathcal{R}}| v_{ar,2}^{\mathcal{R}} (\sin\delta_r e_1 - \cos\delta_r e_2) \\ F_k^{\mathcal{B}} \approx \lambda_k \dfrac{C_k^L(\alpha_k)}{\cos\alpha_k} |\overrightarrow{v}_{ak}|^2 e_2 = -2\lambda_k c_1^k |v_{ak}^{\mathcal{B}}| v_{ak,2}^{\mathcal{B}} e_2 \end{cases} \quad (12)$$

The approximations made in (12) also indicate that the aero(hydro)-dynamic forces acting on the sail, rudder and keel are approximately orthogonal to their average planes. This approximation can also be found in [1,6].

Then, using Eqs. (2), (5), (7), and the approximations in (12), the aero(hydro)-dynamic torques are simplified as:

$$\begin{cases} \tau_s^{\mathcal{B}} = ((r_s - l_s\cos\delta_s)e_1 - l_s\sin\delta_s e_2 + h_s e_3) \times F_s^{\mathcal{B}} \\ \quad \approx 2\lambda_s c_1^s |v_{as}^{\mathcal{S}}| v_{as,2}^{\mathcal{S}} (h_s\cos\delta_s e_1 + h_s\sin\delta_s e_2 + (l_s - r_s\cos\delta_s)e_3) \\ \tau_r^{\mathcal{B}} = (-(r_r + l_r\cos\delta_r)e_1 - l_r\sin\delta_r e_2 - h_r e_3) \times F_r^{\mathcal{B}} \\ \quad \approx 2\lambda_r c_1^r |v_{ar}^{\mathcal{R}}| v_{ar,2}^{\mathcal{R}} (-h_r\cos\delta_r e_1 - h_r\sin\delta_r e_2 + (l_r + r_r\cos\delta_r)e_3) \\ \tau_k^{\mathcal{B}} = -h_k e_3 \times F_k^{\mathcal{B}} \approx -2\lambda_k c_1^k h_k |v_{ak}^{\mathcal{B}}| v_{ak,2}^{\mathcal{B}} e_1 \end{cases} \quad (13)$$

We will show next that the general 6-DOF equations of motion (8)–(9) can be greatly simplified to 4-DOF and 3-DOF models under some assumptions and approximations.

### 3.2.2 Simplified 4-DOF Equations of Motion

By approximating the hull to a volume with three mutually perpendicular axes of symmetry, the contributions of the off-diagonal elements in the added mass matrix can be neglected, i.e. $A_{12} \approx A_{21} \approx 0$ and $A_{11}$ and $A_{22}$ are diagonal.

In this case, Eqs. (9) can be rewritten as:

$$\begin{cases} M\dot{v} = -S(\omega)Mv + F_d^{\mathcal{B}} + F_{res.}^{\mathcal{B}} + F_s^{\mathcal{B}} + F_r^{\mathcal{B}} + F_k^{\mathcal{B}} \\ J\dot{\omega} = -S(\omega)J\omega + \tau_d^{\mathcal{B}} + \tau_{res.}^{\mathcal{B}} + \tau_s^{\mathcal{B}} + \tau_r^{\mathcal{B}} + \tau_k^{\mathcal{B}} \end{cases} \quad (14)$$

with $M := m_0 I_3 + A_{11} = \mathrm{diag}(m_{11}, m_{22}, m_{33})$ and $J := J_0 + A_{22}$.

In order to derive a 4-DOF simplified model, let us assume that the translational motion along $\overrightarrow{k}_0$ direction and the pitch rotational motion are negligible w.r.t. other motions. This leads to the approximations $x_3 = \dot{x}_3 = 0$ and $\theta = \dot{\theta} = 0$. The assumption on the pitch motion can be justified in practice due to the fact that the restoring level arm related to the pitch motion is sufficiently large w.r.t. the one related to the roll motion.

Under these approximations, the rotation matrix $R$ can be simply expressed as a product of a yaw and a roll rotation matrix, i.e. $R = R_\psi R_\phi$, with:

$$R_\psi := \begin{bmatrix} \cos\psi & -\sin\psi & 0 \\ \sin\psi & \cos\psi & 0 \\ 0 & 0 & 1 \end{bmatrix}, \quad R_\phi := \begin{bmatrix} 1 & 0 & 0 \\ 0 & \cos\phi & -\sin\phi \\ 0 & \sin\phi & \cos\phi \end{bmatrix}$$

On the other hand, the fact that $\theta = \dot{\theta} = 0$ leads to the following relations between the angular velocities and the time-derivative of the roll and yaw Euler angles [13]:

$$\begin{cases} \dot{\phi} = \omega_1 \\ \dot{\psi} = \omega_3(\cos\phi)^{-1} \\ \omega_2 = \omega_3 \tan\phi \end{cases} \Rightarrow \begin{cases} \ddot{\phi} = \dot{\omega}_1 \\ \ddot{\psi} = \dot{\omega}_3(\cos\phi)^{-1} + \omega_1\omega_3 \tan\phi(\cos\phi)^{-1} \end{cases}$$

Besides, the relation $\dot{x}_3 = 0$ can be rewritten as:

$$e_3^\top R_\psi R_\phi v = v_2 \sin\phi + v_3 \cos\phi = 0 \;\Rightarrow\; v_3 = -v_2 \tan\phi \tag{15}$$

The assumption on the vertical motion also implies that $\overrightarrow{F}_B = -\overrightarrow{F}_G$ leading to $\overrightarrow{F}_{res.} = \overrightarrow{0}$. The restoring torque can also be approximated by $\tau^{\mathcal{B}}_{res.} = -mgl_\phi \sin\phi e_1$, with a constant restoring level arm $l_\phi > 0$.

The longitudinal and lateral velocities $V_{long.}$, $V_{lat.}$ of the sailboat are defined as:

$$V := \begin{bmatrix} V_{long.} \\ V_{lat.} \\ 0 \end{bmatrix} := R_\psi^\top \dot{x} = R_\phi v = \begin{bmatrix} v_1 \\ v_2\cos\phi - v_3\sin\phi \\ v_2\sin\phi + v_3\cos\phi \end{bmatrix} = \begin{bmatrix} v_1 \\ v_2(\cos\phi)^{-1} \\ 0 \end{bmatrix}$$

where the last equality is obtained using (15). The dynamics of $V$ satisfy:

$$\begin{aligned} \dot{V} &= R_\phi \dot{\phi} S(e_1) v + R_\phi M^{-1}(-S(\omega)Mv + F_d^{\mathcal{B}} + F_s^{\mathcal{B}} + F_r^{\mathcal{B}} + F_k^{\mathcal{B}}) \\ &= \omega_1 S(e_1) V - R_\phi M^{-1} S(\omega) M R_\phi^\top V + R_\phi M^{-1}(F_d^{\mathcal{B}} + F_s^{\mathcal{B}} + F_r^{\mathcal{B}} + F_k^{\mathcal{B}}) \end{aligned}$$

which yields:

$$\begin{cases} \dot{V}_{long.} = -e_1^\top M^{-1} S(\omega) M R_\phi^\top V + e_1^\top M^{-1}(F_d^{\mathcal{B}} + F_s^{\mathcal{B}} + F_r^{\mathcal{B}} + F_k^{\mathcal{B}}) \\ \dot{V}_{lat.} = -e_2^\top R_\phi M^{-1} S(\omega) M R_\phi^\top V + e_2^\top R_\phi M^{-1}(F_d^{\mathcal{B}} + F_s^{\mathcal{B}} + F_r^{\mathcal{B}} + F_k^{\mathcal{B}}) \end{cases} \tag{16}$$

### 3.2.3 Simplified 3-DOF Equations of Motion

Now, we provide a more simplified 3-DOF model for control design purposes by further assuming that the roll rotational motion can also be neglected, i.e. $\phi = \dot{\phi} = 0$. This assumption is well satisfied for particular design of sailboats for which the restoring torque $\overrightarrow{\tau}_{res.}$ dominates all the other external torques

along the roll and pitch axes. Also, considering a null roll angle leads to maximize forces and torques since they are proportional to $\cos\phi$ [9,14]. Using this additional assumption and the approximation $m_{22} \approx m_{33}$, one deduces from Eq. (16) that the translational dynamics satisfy:

$$\begin{cases} m_{11}\dot{V}_{long.} = F^{\mathcal{B}}_{d,1} + F^{\mathcal{B}}_{s,1} + F^{\mathcal{B}}_{r,1} + F^{\mathcal{B}}_{k,1} + m_{22}\omega_3 V_{lat.} \\ m_{22}\dot{V}_{lat.} = F^{\mathcal{B}}_{d,2} + F^{\mathcal{B}}_{s,2} + F^{\mathcal{B}}_{r,2} + F^{\mathcal{B}}_{k,2} - m_{11}\omega_3 V_{long.} \end{cases} \tag{17}$$

The rotational dynamics is approximately given by:

$$\begin{cases} \dot{\psi} = \omega_3 \\ J_{33}\ddot{\psi} = \tau^{\mathcal{B}}_{d,3} + \tau^{\mathcal{B}}_{s,3} + \tau^{\mathcal{B}}_{r,3} + \tau^{\mathcal{B}}_{k,3} \end{cases} \tag{18}$$

If the approximations given in (12) and (13) are further used, one also ensures that $F^{\mathcal{B}}_{k,1} \approx \tau^{\mathcal{B}}_{k,3} \approx 0$, $\tau^{\mathcal{B}}_{s} \approx 2\lambda_s c^s_1 |v^{\mathcal{S}}_{as}| v^{\mathcal{S}}_{as,2}(l_s - r_s\cos\delta_s)$ and $\tau^{\mathcal{B}}_{r} \approx 2\lambda_r c^r_1 |v^{\mathcal{R}}_{ar}| v^{\mathcal{R}}_{ar,2}(l_r + r_r\cos\delta_r)$.

## 4 Heading Control and Sail's Angle Computation

The control design for sailboat's heading and longitudinal motion is considered based on the simplified 3-DOF model proposed previously. In the following, they are decoupled and studied separately.

### *4.1 Heading Control Design*

Controlling the sailboat's heading cannot be assigned independently to the rudder's angle $\delta_r$ in all circumstances. In fact, this can be done only if the component around the $\overrightarrow{k}_0$ axis of the torque generated by the rudder is unbounded. However, this is obviously not true since this torque component is approximately proportional to the square of the norm of the rudder's apparent velocity $\overrightarrow{v}_{ar}$, and thus tends to zero if the apparent velocity $\overrightarrow{v}_{ar}$ vanishes. Therefore, the coordination between the sail's and rudder's angles would be necessary for the success of a given mission. This is the topic of our future work. In the current study we make the assumption that the torque produced by the rudder can compensate all other external torques around the $\overrightarrow{k}_0$ axis. Thus, for control design let us simply consider the following second-order system:

$$\ddot{\psi} = u + c(t) \tag{19}$$

with $u := \tau^{\mathcal{B}}_{r,3}/J_{33}$ the control input assumed to be unbounded for control design purpose, and $c(t) := (\tau^{\mathcal{B}}_{s,3} + \tau^{\mathcal{B}}_{k,3} + \tau^{\mathcal{B}}_{d,3})/J_{33}$ the perturbation term

assumed to be slowly time-varying (i.e. $\dot{c} \approx 0$) so that it can be compensated by an integral action.

Let $\psi_r$ be the reference heading angle to be stabilized. Then, the control objective may be considered as the stabilization of $\psi$ about $\psi_r$, or equivalently the stabilization of the error angle $\tilde{\psi} := \psi - \psi_r$ about zero. However, since the heading evolves on a circle, there is no distinction between $\tilde{\psi}$ and $\tilde{\psi} + k2\pi$, with $k \in \mathbb{N}$, and winding problem may occur. Therefore, it is geometrically more relevant to stabilize $\sin\tilde{\psi}$ about zero.

The control design is based on the backstepping procedure. Consider the first storage function $\mathcal{V}_1 = 1 - \cos(\tilde{\psi})$. By choosing a desired value for $\omega_3$ as $\omega_{3,d} = -k_1 \sin(\tilde{\psi}) + \dot{\psi}_r$, with $k_1$ a positive gain, one deduces:

$$\begin{aligned}\dot{\mathcal{V}}_1 &= \sin(\tilde{\psi})(\omega_3 - \dot{\psi}_r) = \sin(\tilde{\psi})(\omega_{3,d} - \dot{\psi}_r) + \sin(\tilde{\psi})(\omega_3 - \omega_{3,d}) \\ &= -k_1 \sin^2(\tilde{\psi}) + \sin(\tilde{\psi})(\omega_3 - \omega_{3,d})\end{aligned}$$

Next, consider the second storage function $\mathcal{V}_2 = \mathcal{V}_1 + (1/2k_2)(\omega_3 - \omega_{3,d})^2$. One verifies that the time-derivative of $\mathcal{V}_2$ satisfies:

$$\dot{\mathcal{V}}_2 = -k_1 \sin^2(\tilde{\psi}) + \frac{1}{k_2}(\omega_3 - \omega_{3,d})(u + c - \dot{\omega}_{3,d} + k_2 \sin(\tilde{\psi})) \tag{20}$$

The disturbance term $c$ is unknown but can be compensated by its estimate $\hat{c}$ whose dynamics are given by:

$$\dot{\hat{c}} = k_4(\omega_3 - \omega_{3,d}) \ , \ \hat{c}(0) = 0 \tag{21}$$

with $k_4$ a positive gain. Then, by choosing the control input:

$$u = -k_2 \sin(\tilde{\psi}) - k_3(\omega_3 - \omega_{3,d}) + \dot{\omega}_{3,d} - \hat{c} \tag{22}$$

with $k_3$ a positive gain and $\dot{\omega}_{3,d} = -k_1 \cos(\tilde{\psi})(\omega_3 - \dot{\psi}_r) + \ddot{\psi}_r$, one verifies that the time-derivative of the candidate Lyapunov function $\mathcal{V}$ defined as:

$$\mathcal{V} := \mathcal{V}_2 + \frac{k_2}{2k_4}(c - \hat{c})^2 = (1 - \cos(\tilde{\psi})) + \frac{1}{2k_2}(\omega_3 - \omega_{3,d})^2 + \frac{k_2}{2k_4}(c - \hat{c})^2$$

satisfies (using Eqs. (20), (21)):

$$\dot{\mathcal{V}} = -k_1 \sin^2(\tilde{\psi}) - (k_3/k_2)(\omega_3 - \omega_{3,d})^2 \leq 0$$

From here, by application of LaSalle's theorem one deduces that $\dot{\mathcal{V}}$ converges to zero, which in turn implies the convergence of $\sin\tilde{\psi}$ to zero and of $\omega_3$ to $\dot{\psi}_r$. In fact, the convergence of $\sin\tilde{\psi}$ to zero implies that $\tilde{\psi}$ converges to either $k2\pi$ or $\pi + k2\pi$. In practice, this is not a problematic issue since the equilibrium $\tilde{\psi} = \pi + k2\pi$ is unstable and the good equilibrium $\tilde{\psi} = k2\pi$ is stable, i.e. the equilibrium $(\tilde{\psi}, \omega, \hat{c}) = (k2\pi, \dot{\psi}_r, c)$ is almost globally stable.

Now, it matters to determine the real control input for the rudder, i.e. the angle $\delta_r$, as a function of the intermediary control variable $u$ (see Eq. (22)). This is a nonlinear control allocation problem that necessitates further studies. Here, in order to deal with this problem we introduce some approximations. First, we assume that there is no water current, i.e. $\overrightarrow{v}_c = \overrightarrow{0}$. Secondly, the contribution of the rotation motion is negligible w.r.t. the translational motion in the computation of the apparent velocity $\overrightarrow{v}_{ar}$. Finally, the influence of the rudder dynamics on the sailboat is small so that the term dependent upon $\dot{\delta}_r$ in the definition (3) of $\overrightarrow{v}_{ar}$ can be neglected. Thus, in the first approximation one has $\overrightarrow{v}_{ar} \approx \overrightarrow{v}$. Besides, in practice the distance $l_r$ is often very small w.r.t. $r_r$ (i.e., $l_r \ll r_r$). We also assume that the sailboat's lateral velocity is small w.r.t. its longitudinal velocity. Therefore, with a good approximation one verifies that:

$$\tau^{\mathcal{B}}_{r,3} \approx -\lambda_r c^r_1 r_r |v|^2 \sin(2\delta_r)$$

and deduces:

$$\delta_r = -\frac{1}{2}\text{arsin}\left(\text{sat}_1\left(\frac{J_{33}u}{\lambda_r c^r_1 r_r |v|^2}\right)\right)$$

with the classical saturation function $\text{sat}_\Delta(x) := x\min(1, \Delta/|x|)$, $\forall x \in \mathbb{R}$.

## *4.2 Sail's Optimum Angle Computation*

The stability limit of the previous heading controller depends on the bounds of the rudder torque which, in turn, is roughly proportional to the square of the boat's velocity. Thus, maximizing this velocity by choosing an optimum sail's angle is of primary concern. This will be achieved by assuming that the maximum longitudinal force generated by the sail will lead to a maximum longitudinal speed of the sailboat.

This can be done by maximizing $F^{\mathcal{B}}_{s,1}$. Let us calculate such an optimum value of $\delta_s$. From Eq. (12) and using the assumption of (11) one obtains

$$F^{\mathcal{B}}_{s,1} = 2c^s_1 \lambda_s |v^{\mathcal{B}}_{as}| \left(-(\sin\delta_s)^2 v^{\mathcal{B}}_{as,1} + \sin\delta_s \cos\delta_s v^{\mathcal{B}}_{as,2}\right)$$

One obtains:

$$\frac{\partial F^{\mathcal{B}}_{s,1}}{\partial \delta_s} = -2c^s_1 \lambda_s |v^{\mathcal{B}}_{as}| \sin(2\delta_s - \beta)$$

with $\beta = \text{atan2}\left(v^{\mathcal{B}}_{as,2}, v^{\mathcal{B}}_{as,1}\right)$. The optimal condition leads to $\frac{\partial F^{\mathcal{B}}_{s,1}}{\partial \delta_s} = 0$ which yields $\delta^{opt}_s = \beta/2 + k\pi/2$ with $k \in \{0, 1, 2, 3\}$. These four values represent two positive and two negative peaks of $F^{\mathcal{B}}_{s,1}$. The peak of $F^{\mathcal{B}}_{s,1}$ can be calculated to determine $\delta^{max}_s$ the best new configuration (i.e. realistic value of $\delta_s$ that lead to a positive speed).

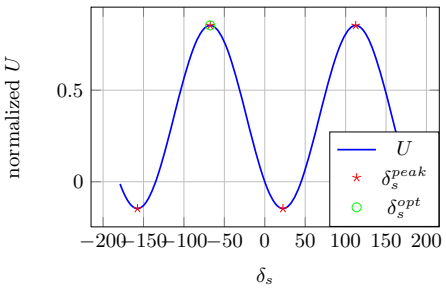


**Fig. 2** Variation of the longitudinal force as a function of $\delta_s$; 4 peaks are found: two negatives two positives. One of the positive peaks is unrealizable $|\delta_s| > 90\,\text{deg}$.

A major drawback of this algorithm is that it does not take into account $F^{\mathcal{B}}_{s,2}$, which may be important at $\delta_s^{opt}$, thus generating an important leeway. Besides, the yaw torque generated by $F_s$ at the chosen $\delta_s$ angle may become very large and cannot be compensated by the rudder.

## 5 Simulation Results

The model described in 3.2.3 and both trimming algorithm and heading controller have been implemented using Matlab and a variable-step solver with a maximum time step of $0.5s$.

To test this model, a first simulation set is done disabling trimming algorithm, using a fixed real wind speed but different real wind direction and setting different values of $\delta_s$ . Rudder's controller with $k_4 = 0$ is used to maintain the desired heading. Speed's polar diagram is then reconstructed as the one that embrace curves from the simulations (fig. 3). One can observe that when the boat attempts to navigate in irons, velocity decreases and reaches zero. In this reconstructed diagram, one can notice that the maximum velocity is reached when sailing downwind. This is due to simulator constants that may not be well tuned.

The heading and speed response to a sudden change of heading reference are illustrated fig 4. In this case, the wind speed is set to $5\,m/s$ with a coming angle of 0 and both sail's trimming algorithm and rudder's controller are used. Heading reference is first set to $\pi/2$ and is changed to $\pi/4$ at $t = 50\,s$. Simulation is done using the controller with parameters $k_1 = 4$, $k_2 = 1.4$, $k_3 = 2.5$ and $k_4 = 0.2$. As previously mentioned, the term $c(t)$ of Eq. (19) includes torque from both sail and hull and is assumed to be varying slowly. In the case where these torques can directly be measured or estimated, a feedforward term may be added to the controller in order to obtain a faster response of the system.

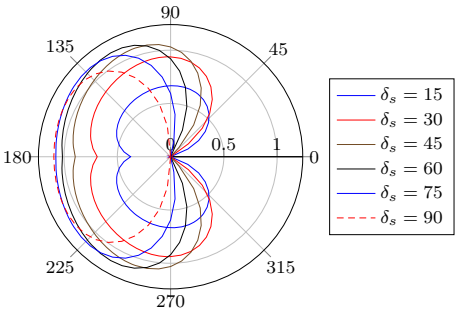


**Fig. 3** Speed's polar diagram as a function of $\delta_s$ at wind speed of $5[m/s]$

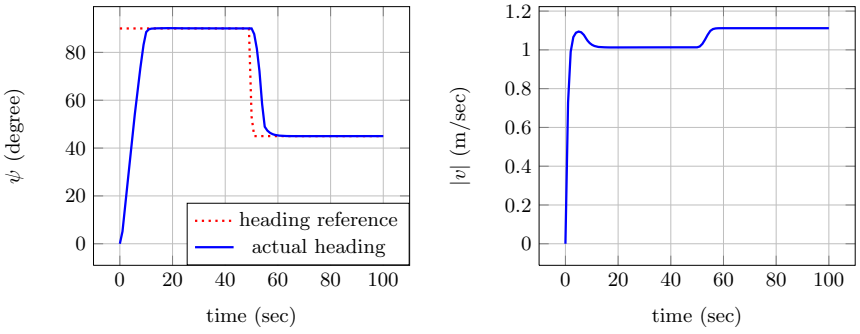


(a) Evolution of boat's heading

(b) Evolution of boat's speed

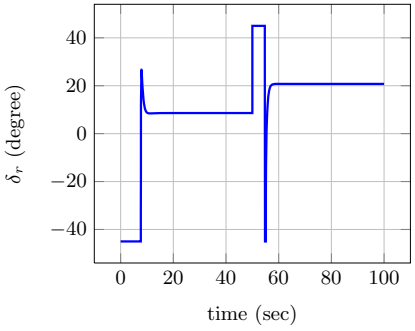


(c) Evolution of input control

**Fig. 4** Response of the system with $\psi_r = \frac{\pi}{2}$ for $t < 50\,s$, $\psi_r = \frac{\pi}{4}$ elsewhere

## 6 Conclusion

Based on a general 6-DOF dynamic model, a simplified 3-DOF ($x-y$ displacement and yaw rotation) sailboat's model has been derived and implemented

on a computer program. This 3-DOF model has been used to design a new heading control law. The controller acts on yaw angle to maintain a desired heading no matter the route direction is. Notice that this controller reaches its limit when boat's velocity is too low because the generated rudder's torque (approximately proportional to the square of the boat velocity) is not sufficient to counter the sail's torque and other disturbances. A sail trimming algorithm is also presented to compute an optimal sail's angle from lift and drag curves, maximizing longitudinal force in order to maximize longitudinal speed. This assertion hold true only for boats with few leeway. Besides, since no verification is done on the torque generated when using this optimal angle, the resulting torque may become too large to be compensated by the rudder, i.e. the yaw controllability is loss. Our future works will focus on designing new controllers overcoming these drawbacks and taking into account roll effect, implementing the 4-DOF and the 6-DOF models and finally comparing their simulation results with real sailboat tests.

## References

1. Briere, Y.: IBOAT: an autonomous robot for long-term offshore operation. In: The 14th IEEE Mediterranean Electrotechnical Conference, MELECON 2008, pp. 323–329 (2008), doi:10.1109/MELCON.2008.4618455
2. Cruz, N., Alves, J.: Autonomous sailboats: An emerging technology for ocean sampling and surveillance. In: MTS/IEEE OCEANS (2008)
3. Elkaim, G.: The atlantis project: A gps-guided wing-sailed autonomous catamaran. Journal of the Institute of Navigation 53, 237–247 (2006)
4. Erckens, H., Busser, G.A., Pradalier, C., Siegwart, R.: Avalon: Navigation strategy and trajectory following controller for an autonomous sailing vessel. IEEE Robotics Automation Magazine 17(1), 45–54 (2010)
5. Fossen, T.I.: Handbook of Marine Craft Hydrodynamics and Motion Control. Wiley-Blackwell (2011)
6. Jaulin, L., Bars, F.L., Clement, B., Gallou, Y., Menage, O., Reynet, O., Sliwka, J., Zerr, B.: Suivi de route pour un robot voilier. In: CIFA 2012, pp. 695–702 (2012), http://hal-ensta-bretagne.archives-ouvertes.fr/hal-00728390
7. Khalil, H.K.: Nonlinear Systems, 3rd edn. Prentice-Hall (2001)
8. Neal, M.: A hardware proof of concept of a sailing robot for ocean observation. IEEE Journal of Oceanic Engineering 31(2), 462–469 (2006)
9. van Oossanen, P.: Theoretical estimation of the influence of some main design factors on the performance of international twelve meter class yachts. In: Chesapeake sailing yacht Symposium, Annapolis, Maryland (1979)
10. Petres, C., Romero-Ramirez, M.A., Plumet, F., Alessandrini, B.: Modeling and reactive navigation of an autonomous sailboat. In: 2011 IEEE/RSJ International Conference on Intelligent Robots and Systems (IROS), pp. 3571–3576 (2011), doi:10.1109/IROS.2011.6094912

11. Pucci, D., Hamel, T., Morin, P., Samson, C.: Nonlinear control of PVTOL vehicles subjected to drag and lift. In: 2011 50th IEEE Conference on Decision and Control and European Control Conference (CDC-ECC), pp. 6177–6183 (2011), 10.1109/CDC.2011.6160712
12. Stelzer, R., Jafarmadar, K., Hassler, H., Charwot, R., et al.: A reactive approach to obstacle avoidance in autonomous sailing. In: International Robotic Sailing Conference, pp. 33–39 (2010)
13. Stuelpnagel, J.: On the parametrization of the three-dimensional rotation group. SIAM Review 6(4), 422–430 (1964), http://www.jstor.org/stable/2027966, doi:10.2307/2027966
14. Van Oossanen, P.: Predicting the speed of sailing yachts'(93-004). Van Oossanen & Associates, Wageningen, The Netherlands (1993)
15. Viola, I.M.: Downwind sail aerodynamics: A CFD investigation with high grid resolution. Ocean Engineering 36(12-13), 974–984 (2009), http://www.sciencedirect.com/science/article/pii/S0029801809001322, doi:10.1016/j.oceaneng.2009.05.011
16. Xiao, L., Jouffroy, J.: Modeling and nonlinear heading control for sailing yachts. In: OCEANS 2011, pp. 1–6 (2011)